Multiplicity dependence of the pion source in S+A collisions at the CERN SPS

K. Kaimi[1], H. Bøggild[2], J. Boissevain[3], M. Cherney[4], J. Dodd[5], S. Esumi[1],
C.W. Fabjan[6], D.E. Fields[3], A. Franz[6], B. Holzer[6], T.J. Humanic[7], B. Jacak[3],
R. Jayanti[7], H. Kalechofsky[7,a], T. Kobayashi[8,b], Y.Y. Lee[7,c], M. Leltchouk[5],
B. Lörstad[9], N. Maeda[1], A. Medvedev[5], A. Miyabayashi[9], M. Murray[10],
S. Nishimura[1,d], E. Noteboom[4], S.U. Pandey[7], F. Piuz[6], V. Polychronakos[11],
M. Potekhin[5], G. Poulard[6], A. Sakaguchi[1], J. Schmidt-Sorensen[2], J. Simon-Gillo[3],
W. Sondheim[3], T. Sugitate[1], J.P. Sullivan[3], Y. Sumi[1], H. van Hecke[3], W.J. Willis[5],
K. Wolf[10] and N. Xu[3]

Abstract

The emission of pions from relativistic heavy-ion collisions of S+S, S+Ag and S+Pb
at 200 GeV/nucleon is characterized using two-particle interferometry. The multi-
plicity dependence of the pion source parameters near mid-rapidity is studied. The
transversal and longitudinal source parameters, R_t and R_l, show a clear increase
with the particle multiplicity. The multiplicity dependence is weaker than that ex-
pected from a simple model of a freeze-out at a constant density.

(submitted to Zeitschift f. Physik)

[1] Hiroshima University, Higashi-Hiroshima 739, Japan.
[2] Niels Bohr Institute, DK-2100, Copenhagen, Denmark.
[3] Los Alamos National Laboratory, Los Alamos, NM 87545, USA.
[4] Creighton University, Omaha, NE, USA.
[5] Columbia University, New York, NY 10027, USA.
[6] CERN, CH-1211 Geneva 23, Switzerland.
[7] Ohio State University, Columbus, OH 43210, USA.
[8] National Laboratory for High Energy Physics, Tsukuba 305, Japan.
[9] University of Lund, S-22362 Lund, Sweden.
[10] Texas A&M University, College Station, TX 77843, USA.
[11] Brookhaven National Laboratory, Upton, NY 11973, USA.
[a] Now at University of Geneva, Geneva, CH-1211, Switzerland.
[b] Now at Riken Linac Laboratory, Riken, Saitama 351-01, Japan.
[c] Now at GSI Laboratory, Darmstadt, D-6100, Germany.
[d] Now at University of Tsukuba, Tsukuba 305, Japan.

1   Introduction

The space-time evolution of the particle emitting source created by relativistic heavy-ion collisions can be investigated by Bose-Einstein interferometry [1, 2]. The primary motivation of interferometry studies is to extract information on the space and time extent of particle emission points from relativistic heavy-ion collisions. In strongly interacting matter at the high energy densities achieved, the quark gluon plasma may be formed [3, 4]. Recently, Bose-Einstein interferometry measurements have been performed in hadron-hadron and nucleus-nucleus collisions to study the mechanism of particle production [5, 6, 7, 8, 9, 10].

Since the system we are observing is a dynamical system with fast expansion, strong re-scattering and shadowing, observed interferometric source size parameters are not simple geometrical sizes at the time hadrons cease to interact, or freeze-out, and depend on kinematical parameters such as the transverse momentum p_T, rapidity y, particle species and centrality of the collisions. Systematic measurements of Bose-Einstein interferometry over a wide kinematical region are necessary to separate the dynamical effects and the intrinsic physical parameters.

The NA44 collaboration has reported measurements of the Bose-Einstein correlation in central S+Pb collisions at the CERN Super-Proton-Synchrotron (CERN-SPS) [11, 12, 13, 14, 15, 16]. The NA44 measurements cover a wide p_T range for both pion and kaon particle species. In this paper, we report a study of the source parameters for positive pions as a function of particle multiplicity in S+A collisions at 200 GeV per nucleon.

2   Experimental Setup

The layout of the NA44 experiment is shown in Fig.1. Incident sulphur ions of 200 GeV per nucleon from the CERN-SPS accelerator go through the beam Cherenkov counter (CX) [17]. CX is used to identify the sulphur ions by the pulse height which is proportional to Z^2 of the ions. CX is also used to give the start signal for the time-of-flight (TOF) measurement, and has a timing resolution of ~30 ps. A plastic scintillation veto counter (CXV) with a 1 cm diameter hole is installed behind CX to eliminate events from the beam halo.

The target is mounted on a support in the dipole magnet (D1). The target is a disk of 1cm in diameter, with the respective target thickness listed in Table 1. A plastic scintillation counter (T0) is installed just after the target to allow a centrality selection at the trigger level. T0 consists of two rectangular scintillator pieces separated by a 3 mm gap through which non-interacting beam particles pass. The pseudo-rapidity coverage of T0 is approximately 1.3 to 3.5. A highly segmented silicon pad detector, with 8 radial and 24 azimuthal sectors, measures the charged particle multiplicity in the pseudo-rapidity range from 1.5 to 3.3.

Particles produced by interactions in the target area are detected by the NA44 focusing spectrometer. The spectrometer consists of three dipole magnets (D1, D2 and D3) and three super-conducting quadrupole magnets (Q1, Q2 and Q3). The dipole magnets D1 and D2 analyze the momentum of the secondary particles, and the last dipole D3 is

	S	Ag	Pb
Thickness (g/cm^2)	2.0	10.5	1.1
Interaction length	5.8 %	13.9 %	1.0 %

Table 1: Targets used in this analysis.

used for a momentum calibration of the spectrometer. The three quadrupole magnets are employed to optimize the spectrometer acceptance and the momentum resolution for the directional Bose-Einstein correlation measurements. The spectrometer magnets are operated in either a horizontal focusing mode ("horizontal" setting) or a vertical focusing mode ("vertical" setting). The "horizontal" setting enables us to make a Bose-Einstein correlation measurement with 2-dimensional parameterization. For the 3-dimensional analysis, the "horizontal" and the "vertical" settings are combined.

The polarity of the magnetic field, the nominal momentum, and the angle of the spectrometer determine the particle charge, the rapidity acceptance and the p_T window of the spectrometer. In this study, the nominal momentum of 4 GeV/c is used and the spectrometer angle is set to 44 mrad with respect to the incident beam line. In the "horizontal" setting, particles with momenta with $\pm$ 20 % of the nominal momentum pass through the spectrometer. For the "vertical" settings, a larger momentum range is accepted. Fig.2 shows the spectrometer acceptance of pions for the "horizontal" and the "vertical" settings. These spectrometer settings cover the p_T range $p_T \leq 0.4$GeV/c and mid-rapidity ($y_{CMS} = 3.0$). The average values of p_T and rapidity y in the acceptance are 135 MeV/c and 3.72 for the "horizontal" setting and 177 MeV/c and 3.51 for the "vertical" setting.

The secondary particles going through the spectrometer magnets are detected by three scintillator hodoscopes (H1, H2 and H3). The hodoscopes consist of 50 plastic scintillator slats for H1 and H3, and 60 slats for H2 with photomultiplier tubes attached to the top and bottom of each scintillator [18]. The sizes of the plastic scintillators for H1, H2 and H3 are $264 \times 28 \times 1$ mm^3, $200 \times 6 \times 6$ mm^3 and $220 \times 13 \times 10$ mm^3 (height$\times$width$\times$thickness), respectively. The scintillator layers of H2 and H3 hodoscopes are perpendicular to the central line of the spectrometer. The H1 hodoscope is rotated by 85 degrees in the horizontal plane so that the scintillator layer of H1 approximately in the focal plane of the spectrometer. The horizontal position resolutions are ~0.7 mm, ~1.7 mm and ~3.8 mm for H1, H2 and H3, respectively, and the vertical position resolutions are ~10 mm, ~8 mm and ~7 mm, respectively. The H3 hodoscope is used for the TOF measurement together with the CX beam counter. A typical TOF resolution between the CX beam counter and the H3 hodoscope is 95 ps.

Two threshold Cherenkov detectors (C1 and C2) are used for particle identification at the trigger level and also in off-line analyses. Each Cherenkov detector consists of a tank filled with radiator gas with thin aluminum entrance and exit windows, a thin concave mirror and a photomultiplier tube. C1 is filled with freon gas at 2.7 atm and C2 is filled with a mixture of nitrogen and neon gas at 1 atm. At particle momenta of 4 GeV/c, electrons, muons and pions are above threshold in C1, and only electrons in C2. In this study, C2 is used in veto mode to reject electrons, and the signal pulse height from C1 is used to purify pion-pair samples in the off-line analysis. A uranium-scintillator calorimeter (UCAL) located at the end of the NA44 spectrometer, has electromagnetic and hadronic sections and is used to separate hadrons, electrons and muons.

The data used in this analysis were collected with the trigger condition:

$$TRIGGER = CX \cdot \overline{CXV} \cdot T0 \cdot \overline{C2} \cdot H1_{\geq 2} \cdot H2_{\geq 2} \cdot H3_{\geq 2}.$$

The threshold of the T0 pulse height defines the centrality of the triggered events. At least two hit slats on each hodoscope were required to trigger the data acquisition system.

2

S+S $\to 2\pi^+$+X		S+Ag $\to 2\pi^+$+X		S+Pb $\to 2\pi^+$+X	
horizontal	vertical	horizontal	vertical	horizontal	vertical
106k	104k	138k	-	197k	200k

Table 2: Number of pion pair events used in this analysis for each target and each spectrometer setting. The nominal momentum is 4 GeV/c.

3   Data Analysis

Track reconstruction is performed by fitting a straight line to the hit positions of particles on the scintillator hodoscopes. For the H1 hodoscope, one particle may hit multiple hodoscope slats due to the shallow angle between the H1 and tracks. This multiple hit may create a fake second track from a single true track. To avoid such fake tracks, events with two tracks hitting neighboring slats on H1 are rejected. ¿From the position and direction of the track the momentum is calculated by assuming the particle propagated from the target through the known magnetic field. The momentum resolution is mainly determined by multiple scattering of the particles in the target, in the air and in the materials of the detectors. A smaller contribution to the momentum resolution is the finite position resolution of the scintillator hodoscopes. In the two particle interferometry measurement, the resolution of the relative momentum between two particles determines the precision of the interferometric source parameters to be extracted. For pions, the relative momenta Q_{to}, Q_{ts} and Q_l (defined below) typically have resolutions 20 MeV/c, 25 MeV/c and 10 MeV/c, respectively.

The mass-squared of the particle is calculated by combining the reconstructed momentum and the TOF information. Two-pion events are selected by requiring at least two tracks with mass-squared in the region of the pion peak and by requiring a C1 ADC pulse height corresponding to 2 or more pions. Fig.3 shows the cut applied in the mass-squared and the C1 ADC contour plot. The contamination of π^+K^+ and π^+p pairs is estimated to be less than 1 % by fitting the π^+, K^+ and p peaks with Gaussian functions. The total number of reconstructed and identified pion pairs for each nuclear target is summarized in Table 2.

For reconstructed positive pion pairs, a raw correlation function $C_{raw}(\boldsymbol{k_1},\boldsymbol{k_2})$ is calculated as follows:

$$C_{raw}(\boldsymbol{k_1},\boldsymbol{k_2}) = D\frac{N_2(\boldsymbol{k_1},\boldsymbol{k_2})}{N_1(\boldsymbol{k_1})N_1(\boldsymbol{k_2})} \tag{1}$$

where $N_2(\boldsymbol{k_1},\boldsymbol{k_2})$ is the number of pion pairs with momenta $\boldsymbol{k_1}$ and $\boldsymbol{k_2}$, and $N_1(\boldsymbol{k_1})$ is the number of pions with momenta $\boldsymbol{k_1}$. D is a constant containing the difference of normalizations between one-particle and two-particle samples. The practical calculation of the denominator of Eq.(1) is made by the so called "event-mixing method" [19] with the same experimental data used for the numerator calculation. The method cancels out effects of the experimental acceptance and trigger biases. It is well known that there is a residual Bose-Einstein correlation effect in the raw correlation function $C_{raw}(\boldsymbol{k_1},\boldsymbol{k_2})$ due to the event-mixing method. A residual effect of the experimental acceptance is also expected. Further, the Bose-Einstein correlation of identical charged particle pairs is affected by the repulsive Coulomb force between particle pairs. To compare with theoretical correlation functions, the following correction is used to produce a corrected correlation function $C_{corr}(\boldsymbol{k_1},\boldsymbol{k_2})$ [11]:

$$C_{corr}(\boldsymbol{k_1},\boldsymbol{k_2}) = C_{raw}(\boldsymbol{k_1},\boldsymbol{k_2}) \times K_{SPC}(\boldsymbol{k_1},\boldsymbol{k_2}) \times K_{acceptance}(\boldsymbol{k_1},\boldsymbol{k_2}) \times K_{Coul}(\boldsymbol{k_1},\boldsymbol{k_2}) \tag{2}$$

3

The event-mixing method uses one particle of a particle pair to generate a single particle spectrum ($N_1(\boldsymbol{k_1})$), and makes uncorrelated particle pairs ($N_1(\boldsymbol{k_1})N_1(\boldsymbol{k_2})$) from the single particle spectrum. However, the single particle spectrum is distorted by the Bose-Einstein correlation. $K_{SPC}(\boldsymbol{k_1},\boldsymbol{k_2})$ is a factor to correct the distortion of the single particle spectrum, and is calculated by a method described in Ref.[11, 19]. $K_{acceptance}(\boldsymbol{k_1},\boldsymbol{k_2})$ is a correction factor for the effects of the finite acceptance and finite momentum resolution of the spectrometer, and is calculated by a Monte Carlo program with a full simulation of the tracking detectors and multiple scattering. $K_{Coul}(\boldsymbol{k_1},\boldsymbol{k_2})$ is the standard Gamow factor for the correction of the Coulomb repulsive force between two charged pions [20].

The Bose-Einstein correlation is evaluated with the following Gaussian parameterized functions in this analysis:

$$C(Q_t, Q_l) = 1 + \lambda e^{-R_t^2 Q_t^2 - R_l^2 Q_l^2} \tag{3}$$

$$C(Q_{to}, Q_{ts}, Q_l) = 1 + \lambda e^{-R_{to}^2 Q_{to}^2 - R_{ts}^2 Q_{ts}^2 - R_l^2 Q_l^2} \tag{4}$$

where Q_t and Q_l are the components of the momentum difference between two pions perpendicular and parallel the beam axis, respectively. Q_t is further separated into two components Q_{to} and Q_{ts}, where Q_{to} is parallel with the transverse component of the momentum sum of the pion pair ($\boldsymbol{k_\perp} = \boldsymbol{k_{1\perp}} + \boldsymbol{k_{2\perp}}$), and Q_{ts} is perpendicular to. The value of Q_l depends on the reference frame and thus the Lorentz boost along the beam axis. The Longitudinal Center-of-Mass System (LCMS) [21], in which the component of the pair momentum sum along the beam axis ($k_z = k_{1z} + k_{2z}$) is zero, is used as the reference frame in this analysis.

The source parameters (R_t, R_l, R_{to}, R_{ts} and λ) are extracted by correcting C_{raw} with Eq.(2) and then fitting the result to Eqs.(3) and (4). In general, the values of the correction factors in Eq.(2) depend on the source parameters. Several iterations of the correction procedure are performed until the source parameters converge [11, 19]. For the success of the iterative procedure, the parameter dependence of the correction factors must be weak. Further, the convergence of the source parameters to the true χ^2 minimum in the fitting procedure is not trivial. We checked the success of the iterative procedure and the convergence of the source parameters with a χ^2 mapping method. In the χ^2 mapping method, we calculate the correction factors and the value of the χ^2 using mesh points in the parameter space. The χ^2 map obtained from the calculation is fitted by a function of a hyper-surface to smooth out the χ^2 map and to get the χ^2 minimum point in the parameter space. The results from the χ^2 mapping method agree with the results from the iterative procedure within statistical errors.

Both the T0 detector and the silicon pad detector provide information on the charged particle multiplicity of an event. In principle, the silicon detector provides the more accurate measurement of the charged particle multiplicity, however at high beam rates, it becomes susceptible to overlapping events ("pile up"). The T0 detector does not suffer from pile up, and the multiplicity is therefore determined by using the ADC value of the T0 detector. The absolute normalization of the charged particle multiplicity is done by comparing the T0 ADC value and the multiplicity from the silicon pad detector at a low beam intensity. Since the target thicknesses are finite, the probability of having double interactions in the target is not zero, and the double interactions increase the observed particle multiplicity. The effect of the double interactions is estimated to be less than 10 %, and is corrected for with a Monte Carlo simulation. The charged particle multiplicity per unit pseudo-rapidity $dN_{ch}/d\eta$ is calculated at the pseudo-rapidity of 2.7, which is the

4

System	$< dN_{ch}/d\eta >$	λ	R_t	R_l	χ^2/NDF
S+S	20±10	0.54±0.02	2.84±0.17	4.00±0.29	334/398
	44±11	0.59±0.03	3.74±0.20	3.76±0.35	307/398
S+Ag	41±14	0.53±0.03	3.15±0.20	4.97±0.41	332/390
	71±10	0.54±0.03	3.51±0.25	4.11±0.39	357/385
	100±13	0.57±0.03	3.67±0.23	5.07±0.39	405/396
S+Pb	24±10	0.53±0.02	3.07±0.19	3.70±0.30	377/394
	67±13	0.57±0.03	3.71±0.21	4.92±0.37	397/378
	96±9	0.61±0.03	3.80±0.18	4.03±0.33	340/378
	117±12	0.62±0.03	4.32±0.25	4.88±0.37	356/385
Systematic Error		0.02	0.10	0.16	

Table 3: Multiplicity dependence of the pion source parameters with the 2-dimensional parameterization of the correlation function for π^+ pairs. Typical systematic errors are listed at the bottom.

center of the pseudo-rapidity coverage of the silicon pad detector. The systematic error of the absolute normalization of the charged multiplicity is estimated to be about 20 %.

Systematic errors of the source parameters are estimated by changing analysis conditions and refitting the correlation function: (i) the neighboring-slat cut of H1 is extended to H2 and H3, (ii) the momentum resolution in Monte Carlo data is increased by 20 % from the assumed value and (iii) the slope parameter of pion transverse mass ($m_T = \sqrt{m_\pi^2 + p_T^2}$) spectrum of the Monte Carlo data is changed by 30 %. Typical values of overall systematic errors are listed at the bottom in Tables 3 and 4. Further details of the systematic error analysis can be found elsewhere [14].

4   Results

Several sub-samples of data are created to look at the multiplicity dependence of the pion source parameters. We use 2, 3 and 4 multiplicity bins for the S+S, S+Ag and S+Pb data respectively.

First, the multiplicity dependence study is performed with the 2-dimensional correlation function. Fig.4 shows the correlation function C_{corr} projected on the Q_t and the Q_l axes for the 4 multiplicity bins of the S+Pb data. The pion source parameters obtained for all collision system are summarized in Table 3. The errors of the interferometric source parameters are statistical only. The errors of the mean multiplicities mainly comes from the widths of multiplicity cuts, and statistical fluctuation of number of charged particles in the T0 detector acceptance gives minor contribution to the errors. The extracted source parameters R_t, R_l and λ are shown as a function of the charged particle multiplicity in Fig.5.

The transverse pion source parameter, R_t, shows a clear increase with charged particle multiplicity, $dN_{ch}/d\eta$, and has almost the same value at the same particle multiplicity for different targets. This means that the particle multiplicity mainly determines the pion source parameters at freeze-out and the details of initial conditions do not strongly affect the pion source around mid-rapidity. The longitudinal pion source parameter, R_l, also increases with the charged particle multiplicity.

The λ parameter has values around 0.57 and the variation of the values of the λ parameter is about 0.1 over the charged particle multiplicity range from 30 to 120. In pion two-particle interferometry measurements, values of the λ parameter considerably

System	$< dN_{ch}/d\eta >$	λ	R_{to}	R_{ts}	R_l	χ^2/NDF
S+S	20±10	0.55±0.02	3.02±0.13	2.95±0.17	4.01±0.28	5668/5796
	44±11	0.58±0.02	3.82±0.16	3.78±0.26	3.59±0.35	5124/5744
S+Pb	24±10	0.57±0.03	3.39±0.15	2.90±0.19	3.55±0.30	5280/5925
	67±13	0.56±0.03	3.90±0.16	3.14±0.19	4.52±0.33	5524/5976
	96±9	0.60±0.03	3.94±0.15	3.97±0.26	3.82±0.31	5534/5972
	117±12	0.61±0.03	4.69±0.23	3.68±0.32	4.87±0.35	4917/5842
Systematic Error		0.03	0.3	0.3	0.2	

Table 4: Multiplicity dependence of the pion source parameters with the 3-dimensional parameterization of the correlation function for π^+ pairs in the S+S and S+Pb collisions. Typical systematic errors are listed at the bottom.

smaller than 1 have been reported, and effects of the decay of long-lived resonances [22] and the shape of experimental acceptances [16] were proposed as explanations. Further, double interactions in the target slightly decreases the values of the λ parameter in this experiment. This effect of double interactions is estimated with a Monte Carlo calculation to be less than 10 % and is corrected for.

A 3-dimensional analysis of the Bose-Einstein correlation is also performed for the S+S and S+Pb systems. Fig.6 shows the correlation function C_{corr} for the S+Pb data. Fig.7 shows the multiplicity dependence of the source parameters, R_{ts} and R_{to}, from the 3-dimensional analysis. The results are summarized in Table 4.

5   Discussion and Conclusion

The particle multiplicity, dN/dy, around mid-rapidity is roughly proportional to the available energy for particle production. For a linearly expanding system, the total volume is proportional to the cube of the expansion time, and the volume at freeze-out will be proportional to the cube of the time at freeze-out τ_f^3. If the freeze-out occurs at a constant density, the time at freeze-out should be proportional to the cubic root of particle density, $\tau_f \propto (dN/dy)^{1/3}$ [23].

Interferometric source radii parameters depend not only on the geometrical size of the source region at freeze-out, they are also related to the position-momentum correlations at freeze-out. We have earlier studied the dependence of the radii parameters on transverse mass for S+Pb interactions and shown that they are all proportional to $1/\sqrt{m_T}$ in the longitudinal center of mass system [15]. The results from NA35 [6] are consistent with our measurements. This is expected for a linearly expanding large hydrodynamical system with a constant freeze-out temperature T_f where all radii parameters are proportional to $\tau_f \sqrt{T_f/m_T}$ [24]. By studying the multiplicity dependence we can test the proportionality to τ_f, and under certain assumptions estimate its value.

The multiplicity dependence of the transverse, R_t, and longitudinal, R_l, pion source parameters are fitted with the function:

$$R_{t,l} = C \left(\frac{dN_{ch}}{d\eta} \right)^\alpha \tag{5}$$

where C is a normalization constant. The result of the fitting is shown with the curves in Fig.5 and the parameters are listed in Table 5. The multiplicity dependence of the 3-dimensional pion source parameters, R_{to} and R_{ts}, are also fitted with Eq.(5), and the

6

	C	α	χ^2/NDF
R_t	1.77 ± 0.76	0.17 ± 0.10	$5.5/7$
R_l	2.76 ± 1.56	0.11 ± 0.14	$12.3/7$
R_{to}	1.91 ± 0.59	0.17 ± 0.07	$5.4/4$
R_{ts}	1.92 ± 0.73	0.14 ± 0.09	$7.3/4$

Table 5: Parameters obtained from the fitting of the multiplicity dependence with a function $C(dN_{ch}/d\eta)^\alpha$.

result is shown in Fig.7 and listed in Table 5. All values of the α parameter from the fitting are smaller than the value $1/3$ expected from a simple model of freeze-out at a constant density. One explanation of the small values of α is the assumption of the proportionality of the pion source parameters to $\tau_f\sqrt{T_f/m_T}$ is too simple. A multiplicity dependence of the strength of the position-momentum correlation may explain the small values of α. If the strength of the position-momentum correlation increases by about 25 % from $dN_{ch}/d\eta$=30 to 120, the values of α become consistent with $1/3$.

Using the approximate formula $R_{t,l} \approx \tau_f\sqrt{T_f/m_T}$ [24, 25, 26] and an assumption of the value of the freeze-out temperature T_f=140 MeV [27], τ_f is estimated to be 5.0 ± 0.6 fm/c at $dN_{ch}/d\eta$=100, which is consistent with Ref.[6]. Wiedemann et al. [28] made a numerical calculation based on a hydrodynamical model and pointed out the formula $R_{t,l} \approx \tau_f\sqrt{T_f/m_T}$ is not a good approximation in the low p_T region. The model ambiguity may contribute to an additional error in the τ_f estimation.

In conclusion, the multiplicity dependence of the pion source parameters in S+S, S+Ag and S+Pb collisions is studied by the two-particle interferometry technique. The transversal (R_t) and longitudinal (R_l) pion source parameters are independent of the initial nuclei in the interaction and increase with increasing multiplicity. This suggests that the freeze-out process is governed mainly by the particle multiplicity, which is roughly proportional to the energy available for particle production, but the size of the target nuclei. The multiplicity dependence of the pion source parameters is weaker than a multiplicity dependence expected from a simple model of the freeze-out at a constant density and an assumption of a proportionality of pion source parameters to $\tau_f\sqrt{T_f/m_T}$. The pion freeze-out time is estimated to be roughly 5.0 ± 0.6 fm/c at $dN_{ch}/d\eta$=100.

References

[1] R. Hanbury-Brown and R.Q. Twiss, Nature **178** (1956) 1046.

[2] G. Goldhaber et al., Phys. Rev. **120** (1960) 300.

[3] G. Bertsch and G.E. Brown, Phys. Rev. **C40** (1989) 1830.

[4] S. Pratt, Phys. Rev. **D33** (1986) 72.

[5] M. Lahanas et al., NA35 Collab., Nucl. Phys. **A525** (1991) 327c.

[6] Th. Alber et al., NA35 Collab., Institut für Kernphysik Universität Farnkfurt Report No. IKF-HENPG/9-94, 1994; T. Alber et al., NA35 Collab., Z. Phys. **C66** (1995) 77.

[7] C.S. Lindsey et al., E735 Collab., Nucl. Phys. **A544** (1992) 343c.

[8] Y. Akiba et al., E-802 Collab., Phys. Rev. Lett. **70** (1993) 1057.

[9] W.B. Christine et al., Phys. Rev. **C47** (1993) 779.

[10] T. Abbott et al., E-802 Collab., Phys. Rev. Lett. **69** (1992) 1030.

[11] H. Bøggild et al., NA44 Collab., Phys. Lett. **B302** (1993) 510.

[12] J. Sullivan et al., Phys. Rev. Lett. **70** (1993) 3000.

[13] H. Bøggild et al., NA44 Collab., Phys. Lett. **B349** (1995) 386.

[14] H. Beker et al., NA44 Collab., Z. Phys. **C64** (1994) 209.

[15] H. Beker et al., NA44 Collab., Phys. Rev. Lett. **74** (1995) 3340.

[16] D.E. Fields et al., Phys. Rev. **C52** (1995) 986.

[17] N. Maeda et al., Nucl. Instr. Methods **346** (1994) 132.

[18] T. Kobayashi and T. Sugitate, Nucl. Instr. Methods **A287** (1990) 389.

[19] W.A. Zajc et al., Phys. Rev. **C29** (1984) 2173.

[20] M. Gyulassy and S.K. Kauffmann, Nucl. Phys. **A362** (1981) 503.

[21] T. Csörgő and S. Pratt, Workshop on Relativistic Heavy Ion Physics, Central Research Institute Budapest, KFKI-1991-28/A, p.75, and LUND Report No. LU TP 91-10.

[22] P. Grassberger, Nucl. Phys. **B120** (1977) 231.

[23] S. Nagamiya, Nucl. Phys. **A544** (1992) 5c.

[24] T. Csörgő and B. Lörstad, Lund Report No. LUNFD6/(NFFL-7082), 1994.; T. Csörgő and B. Lörstad, Phys. Rev. **C54** (1996) 1390.

[25] Yu.M. Sinyukov, Nucl. Phys. **A498** (1989) 151c.

[26] J.D. Bjorken, Phys. Rev. **D27** (1983) 140.

[27] I.G. Bearden et al., NA44 Collab., CERN Report No. CERN-PPE/96-163.

[28] U.A. Wiedemann, P. Scotto and U. Heinz, Phys. Rev. **C53** (1996) 918.

8

Figure Captions

Fig. 1. A schematic view of the NA44 experimental setup.

Fig. 2. Contour plot of the spectrometer acceptances in the rapidity y and the transverse momentum p_T space. The acceptances for the "horizontal" and the "vertical" settings are shown. The nominal momentum setting is 4 GeV/c and the spectrometer angle is 44 mrad. The center of mass rapidity of the nucleon-nucleon system is about 3.

Fig. 3. Contour plot of the mass-squared and the C1 ADC. To purify the pion-pair sample, the events within the cut (box in the figure) are selected.

Fig. 4. Projections of the 2-dimensional correlation function C_{corr} onto the Q_t (top) and Q_l (bottom) axes are created for the 4 charged particle multiplicity intervals of the S+Pb collisions. The average charged particle multiplicity increases from (a) to (d).

Fig. 5. The extracted pion source parameters R_t, R_l and λ as a function of the charged particle multiplicity $dN_{ch}/d\eta$ for the S+A$\rightarrow 2\pi^+$+X reaction at 200 GeV per nucleon. The curves in the figure are results of the fitting of data points with a function proportional to $(dN_{ch}/d\eta)^\alpha$.

Fig. 6. Projections of the 3-dimensional correlation function C_{corr} onto the Q_{to} (top), Q_{ts} (middle) and Q_l (bottom) axes are created for the 4 charged particle multiplicity intervals of the S+Pb collisions. The average charged particle multiplicity increases from (a) to (d).

Fig. 7. The extracted pion source parameters R_{to} and R_{ts} as a function of the charged particle multiplicity $dN_{ch}/d\eta$ for the S+A$\rightarrow 2\pi^+$+X reaction at 200 GeV per nucleon. The curves in the figure are results of the fitting of data points with a function proportional to $(dN_{ch}/d\eta)^\alpha$.
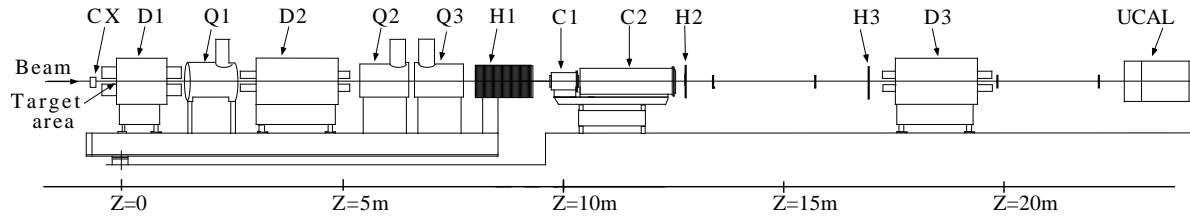
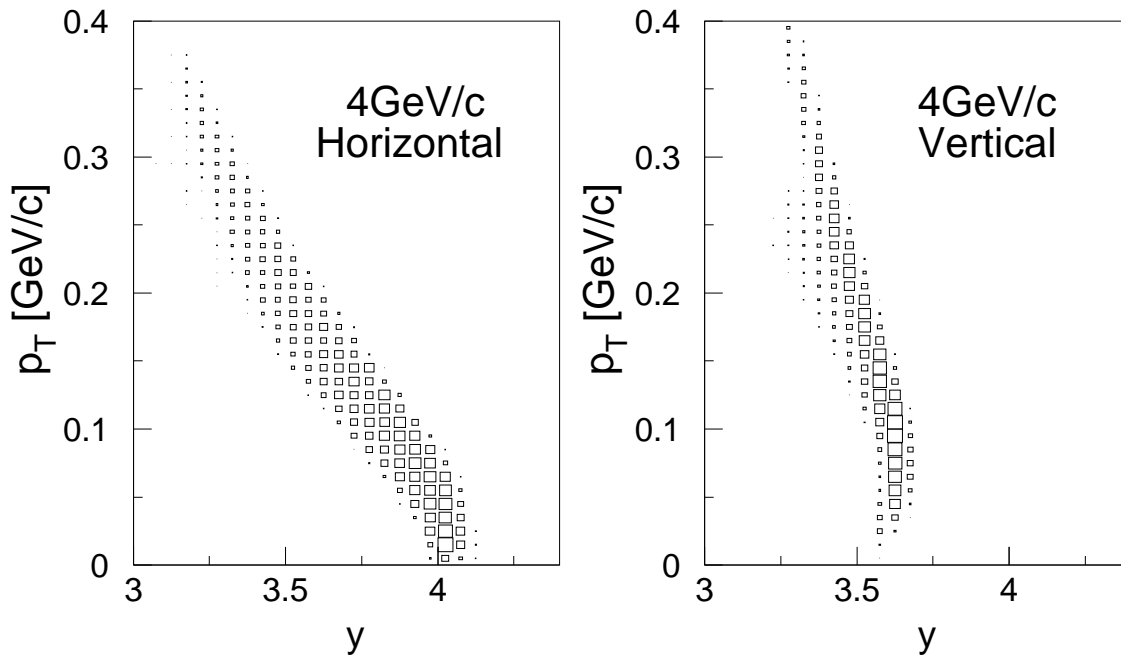Figure 1: A schematic view of the NA44 experimental setup.

Figure 2: Contour plot of the spectrometer acceptances in the rapidity y and the transverse momentum p_T space. The acceptances for the "horizontal" and the "vertical" settings are shown. The nominal momentum setting is 4 GeV/c and the spectrometer angle is 44 mrad. The center of mass rapidity of the nucleon-nucleon system is about 3.
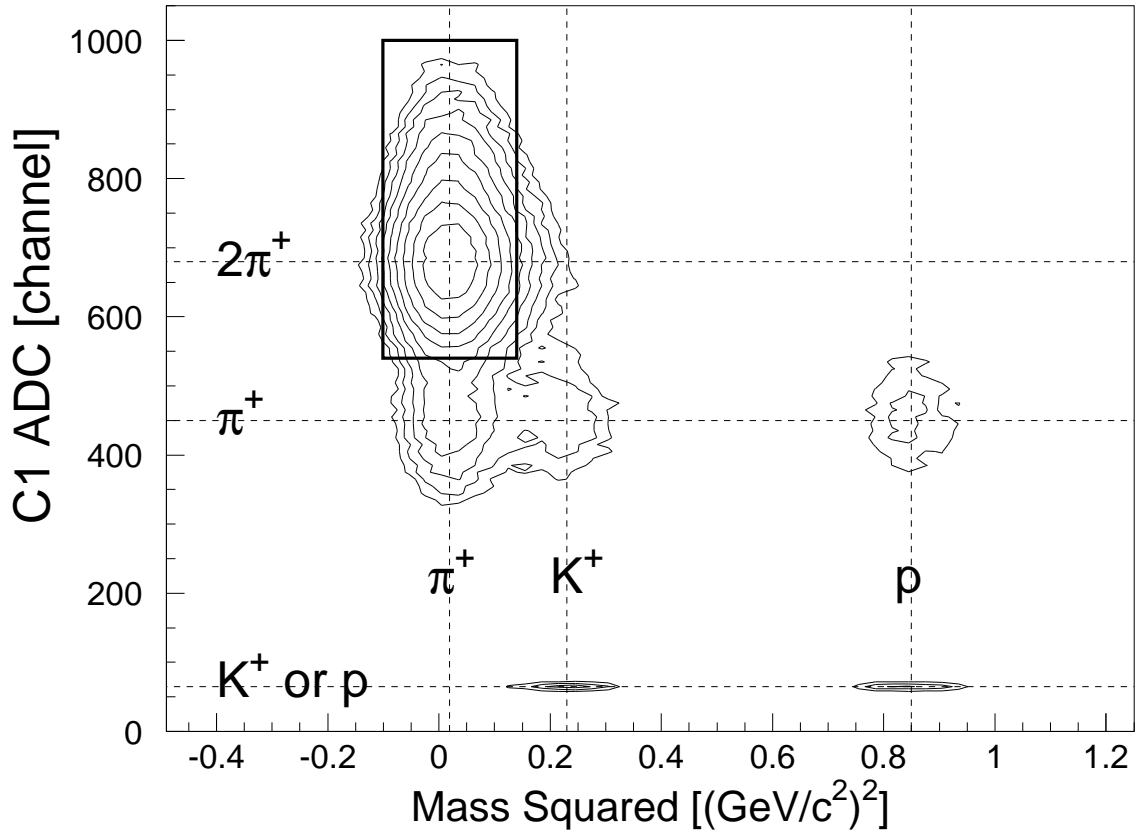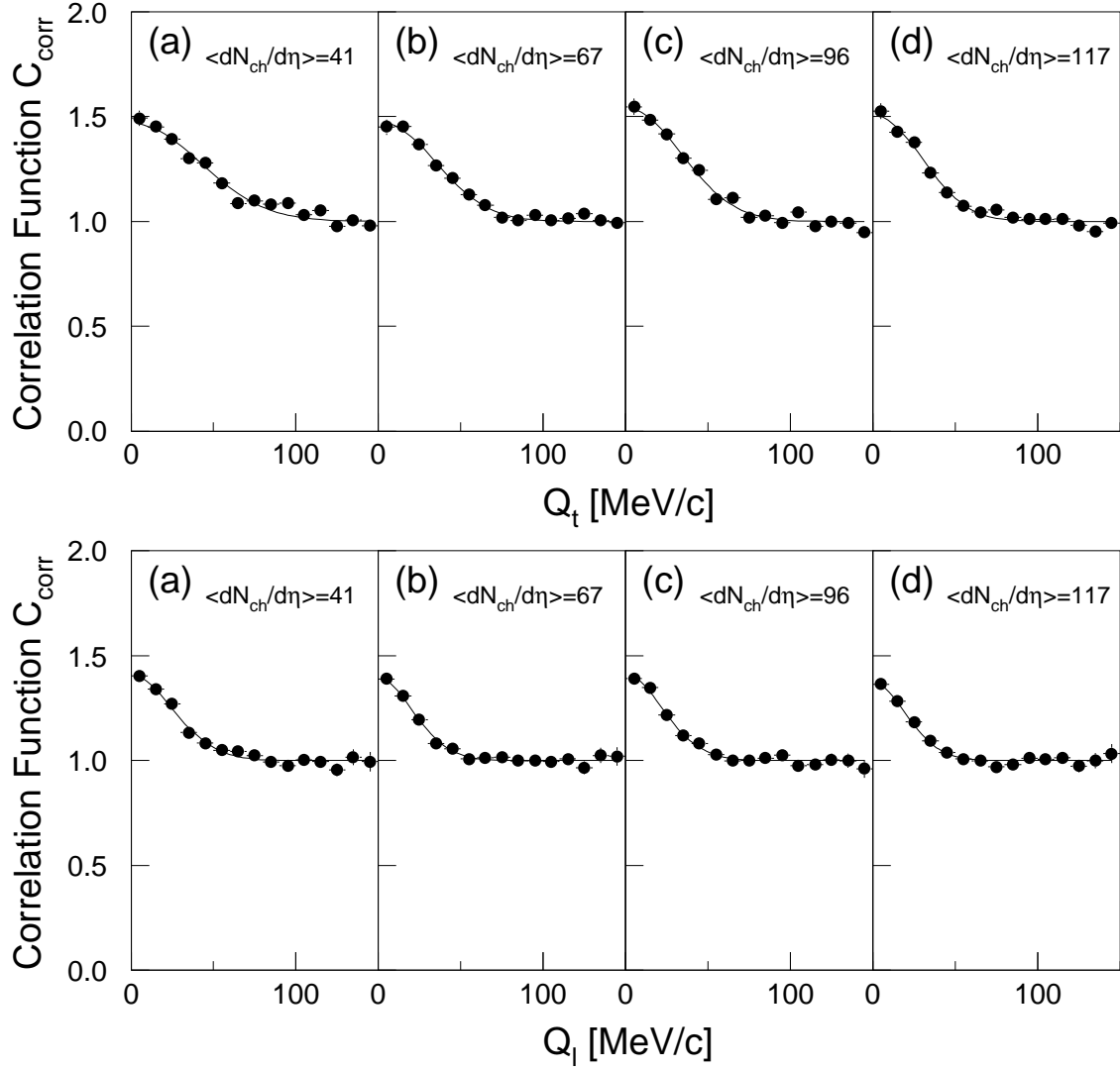
Figure 3: Contour plot of the mass-squared and the C1 ADC. To purify the pion-pair sample, the events within the cut (box in the figure) are selected.

Figure 4: Projections of the 2-dimensional correlation function C_{corr} onto the Q_t (top) and Q_l (bottom) axes are created for the 4 charged particle multiplicity intervals of the S+Pb collisions. The average charged particle multiplicity increases from (a) to (d).
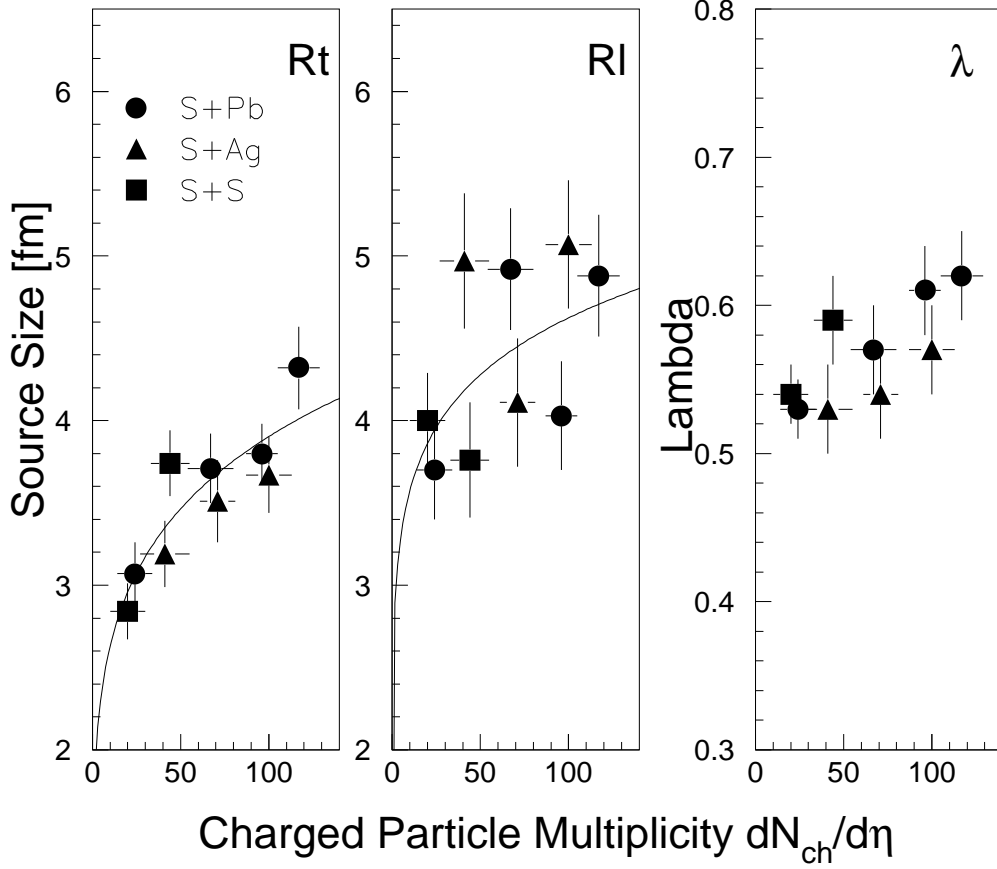
12

Figure 5: The extracted pion source parameters R_t, R_l and λ as a function of the charged particle multiplicity $dN_{ch}/d\eta$ for the S+A→ $2\pi^+$+X reaction at 200 GeV per nucleon. The curves in the figure are results of the fitting of data points with a function proportional to $(dN_{ch}/d\eta)^\alpha$.
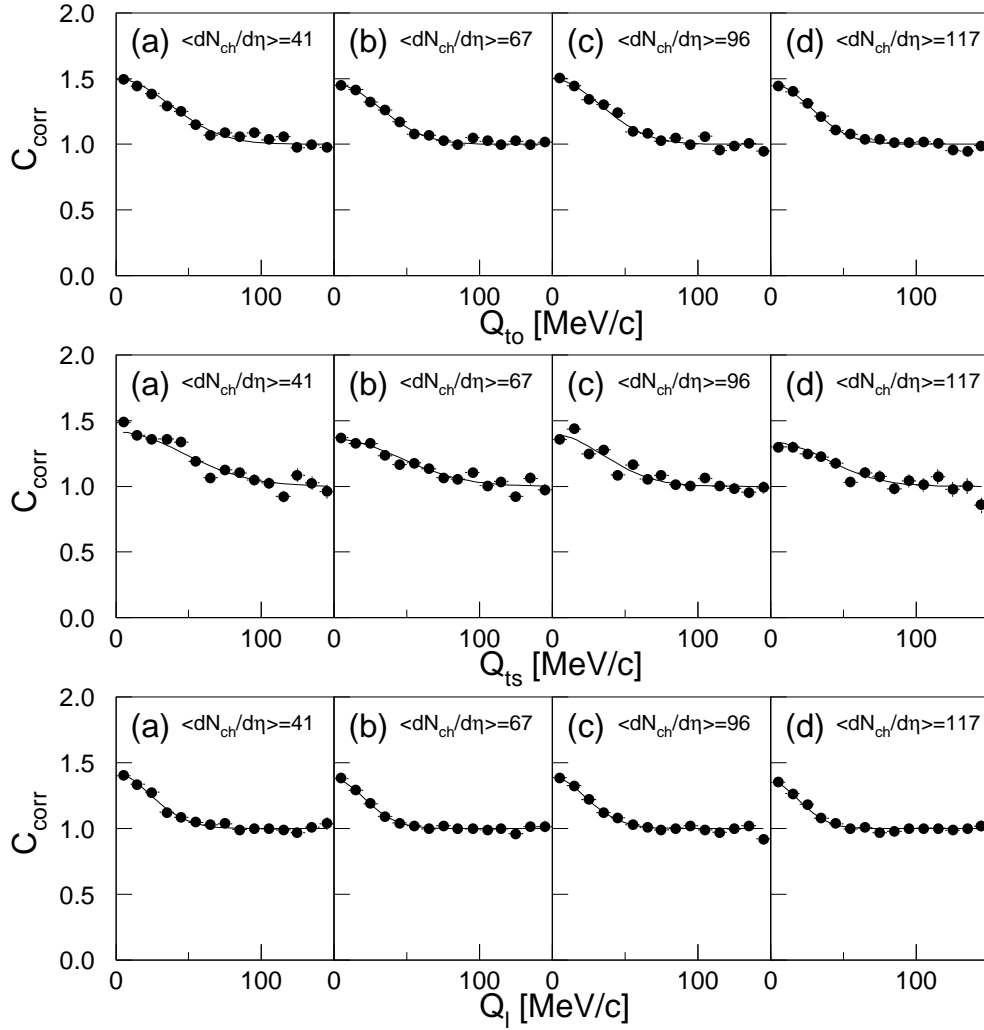
Figure 6: Projections of the 3-dimensional correlation function C_{corr} onto the Q_{to} (top), Q_{ts} (middle) and Q_l (bottom) axes are created for the 4 charged particle multiplicity intervals of the S+Pb collisions. The average charged particle multiplicity increases from (a) to (d).
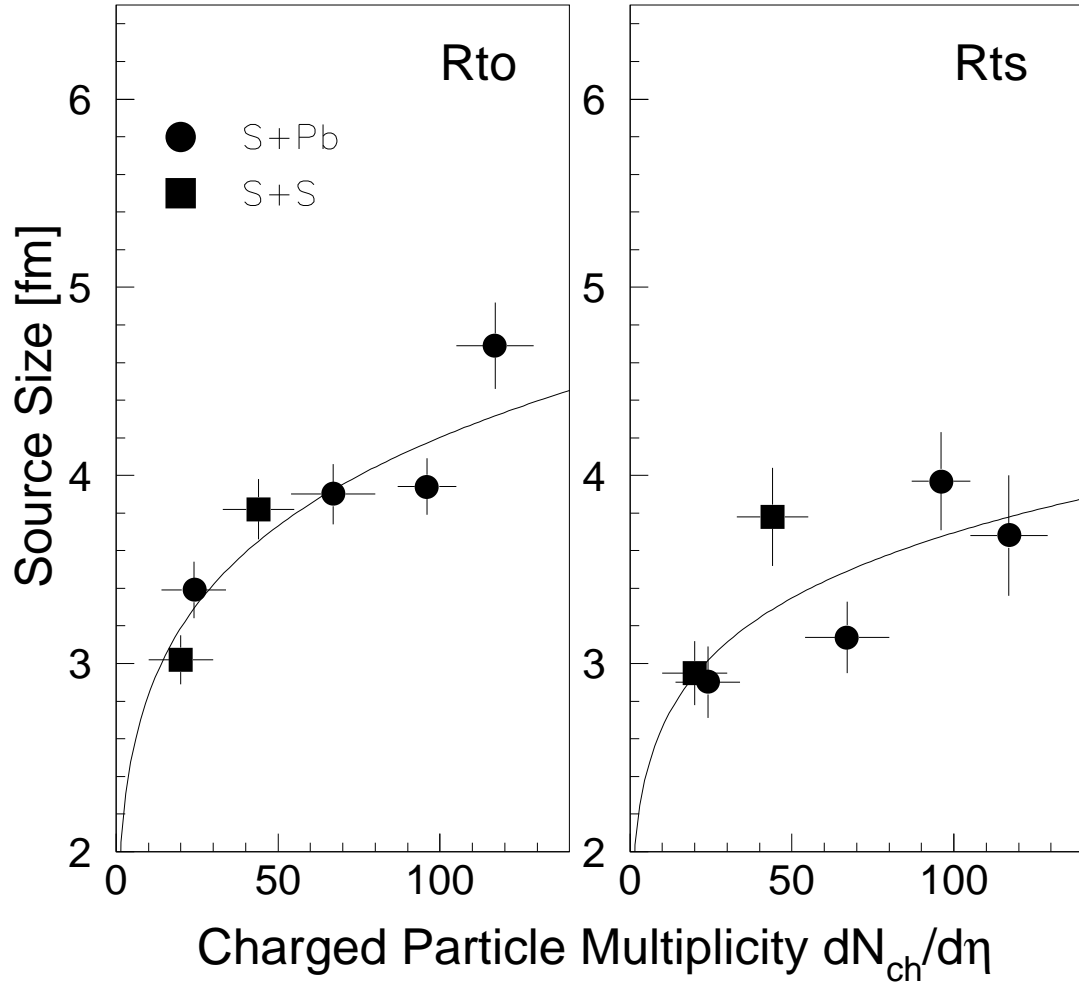
Figure 7: The extracted pion source parameters R_{to} and R_{ts} as a function of the charged particle multiplicity $dN_{ch}/d\eta$ for the S+A→$2\pi^{+}$+X reaction at 200 GeV per nucleon. The curves in the figure are results of the fitting of data points with a function proportional to $(dN_{ch}/d\eta)^{\alpha}$.